



*Dedicated to the memory of  
Professor Ioan Silaghi-Dumitrescu (1950 – 2009)*

## UNSYMMETRICAL DINUCLEAR RHODIUM COMPLEXES WITH ARSANYL- AND PHOSPHANYLARYLTHIOLATO LIGANDS [Rh( $\mu$ -S-2-EPh<sub>2</sub>C<sub>6</sub>H<sub>4</sub>- $\kappa^2$ S,E)<sub>2</sub>Rh(cod)] (E = As, P)

Alexandra HILDEBRAND,<sup>a,b</sup> Menyhárt B. SÁROSI,<sup>a</sup> Peter LÖNNECKE,<sup>b</sup>  
Luminița SILAGHI-DUMITRESCU<sup>a\*</sup> and Evamarie HEY-HAWKINS<sup>b\*</sup>

<sup>a</sup> Faculty of Chemistry and Chemical Engineering, Babeş-Bolyai University, Kogalniceanu 1, RO-400084 Cluj-Napoca, Roumania

<sup>b</sup> Universität Leipzig, Institut für Anorganische Chemie, Johannisallee 29, D-04103 Leipzig, Germany

*Received March 30, 2010*

The heteroditopic ligands 1-EPh<sub>2</sub>-2-SHC<sub>6</sub>H<sub>4</sub> (E = P, As) react with [RhCl(cod)]<sub>2</sub> to give [Rh( $\mu$ -S-2-EPh<sub>2</sub>C<sub>6</sub>H<sub>4</sub>- $\kappa^2$ S,E)<sub>2</sub>Rh(cod)] (cod = 1,5-cyclooctadiene, **1**: E = As, **2**: E = P), in which the two rhodium atoms are bridged by the thiolato groups of the ligands. One rhodium atom is coordinated by both ligands ( $\kappa^2$ S,E) and the other rhodium atom by an additional 1,5-cyclooctadiene molecule, resulting in square-planar coordination geometry of both rhodium(I) centres. Theoretical studies confirmed the existence of metal-metal interactions between the two rhodium atoms of both **1** and **2**. Complex **1** is active in the hydrogenation of olefins.

### INTRODUCTION

Hemilabile ligands are important in homogeneous catalysis, where the lability of a donor group may allow coordination, activation and transformation of a substrate molecule at the metal site. At the same time, the labile donor function stabilises the complex in the absence of a substrate and favours elimination of the product. The presence of a hemilabile ligand in a complex may significantly affect the reactivity of incoming substrates and promote transformations that would otherwise not occur.<sup>1-4</sup>

Endowed with soft and hard donor groups, P,O- and P,N-based ligands are the most studied class of hemilabile functional phosphines. There are numerous examples of metal complexes with P,O ligands that have been used in catalysis.<sup>4</sup> The class of P,S mixed-donor ligands has received increasingly attention and developed rapidly in recent decades,

and several examples for their use in catalysis have been reported.<sup>2,5-13</sup>

Phenylene-bridged phosphinothiols have been prepared previously by an efficient method involving *ortho*-lithiation of lithium thiophenolate developed in 1989.<sup>14</sup> Since then, a number of substituted phosphanylthiols have been prepared, including 1-PPh<sub>2</sub>-2-SHC<sub>6</sub>H<sub>4</sub> (**PSH**), PhP(2-SHC<sub>6</sub>H<sub>4</sub>)<sub>2</sub> (**PS<sub>2</sub>H<sub>2</sub>**) and P(2-SHC<sub>6</sub>H<sub>4</sub>)<sub>3</sub> (**PS<sub>3</sub>H<sub>3</sub>**), reported by E. Block *et al.*<sup>15</sup> The coordination chemistry towards a considerable number of metals has been extensively explored with these ligands (in their deprotonated form). The rhodium(I) carbonyl complex, [Rh{(PS)- $\kappa^2$ S,P}(CO)]<sub>2</sub> containing the deprotonated phosphanylthiolato ligand 1-PPh<sub>2</sub>-2-SHC<sub>6</sub>H<sub>4</sub> (**PSH**), reported by Dilworth *et al.* in 1995, proved to be an efficient catalyst for the carbonylation of methanol to acetic acid.<sup>6</sup>

\* Corresponding author: [lusi@chem.ubbcluj.ro](mailto:lusi@chem.ubbcluj.ro) (L. Silaghi-Dumitrescu) or [hey@uni\\_leipzig.de](mailto:hey@uni_leipzig.de) (E. Hey-Hawkins)

In contrast to the rich chemistry of the phosphanylarylthiolato ligands  $\text{PS}^-$ ,  $\text{PS}_2^{2-}$  and  $\text{PS}_3^{3-}$ , the chemistry of the analogous arsanylarylthiolates  $\text{AsS}^-$ ,  $\text{AsS}_2^{2-}$  and  $\text{AsS}_3^{3-}$  is less well developed. Although a number of examples of transition metal complexes of triorganoarsines which are efficient catalysts in organic synthesis are already known, the combination of an arsenic atom and one or more sulfur atoms in the same ligand is not widely exploited. Catalytic applications may be complicated by the fact that sulfur species are considered to be potential catalyst poisons that cause a substantial decrease in the catalytic activity.<sup>16</sup> However, promotional rather than poisonous effects of sulfur were also reported in selective hydrogenation reactions on supported noble metal catalysts by stabilising the bonding of unsaturated molecules through electronic effects.<sup>17</sup> Furthermore, introduction of a chiral arsenic centre would have an interesting effect on the stereochemistry and enable the potential use of these ligands as chiral auxiliaries for homogeneous asymmetric catalysis to be explored. We report here the synthesis of two rhodium(I) complexes of  $\text{AsS}^-$  and  $\text{PS}^-$ ,  $[\text{Rh}(\mu\text{-S-2-AsPh}_2\text{C}_6\text{H}_4\text{-}\kappa^2\text{S,As})_2\text{Rh}(\text{cod})]$  (**1**) and  $[\text{Rh}(\mu\text{-S-2-PPh}_2\text{C}_6\text{H}_4\text{-}\kappa^2\text{S,P})_2\text{Rh}(\text{cod})]$  (**2**;  $\text{cod} = 1,5\text{-cyclooctadiene}$ ), and the application of **1** in the hydrogenation of olefins.

## EXPERIMENTAL

All manipulations were carried out by standard Schlenk techniques under an atmosphere of dry nitrogen. The NMR spectra were recorded on a Bruker Avance DRX-400 spectrometer.  $^1\text{H}$  and  $^{13}\text{C}$  chemical shifts are quoted in ppm relative to tetramethylsilane. The chemical shifts for  $^{31}\text{P}$  NMR spectra are quoted in ppm at 161.97 MHz relative to external 85%  $\text{H}_3\text{PO}_4$ . The infrared spectra were recorded on a Perkin-Elmer System 2000 FT-IR spectrometer scanning between 400 and 4000  $\text{cm}^{-1}$  using KBr pellets (KBr dried in vacuum, 150 °C,  $10^{-3}$  Torr, 24 h). The samples were prepared in a glovebox. The melting points were determined in sealed capillaries and are uncorrected. The mass spectra were recorded on a VG12-520 mass spectrometer (EI-MS, 70 eV, 200 °C), and elemental analysis was performed with a Vario EL - Heraeus.  $[\{\text{RhCl}(\text{cod})\}_2]$ ,<sup>18</sup>  $\text{Ph}_2\text{AsCl}$ ,<sup>19</sup> and 1-E $\text{Ph}_2$ -2-SHC $_6\text{H}_4$  (E = P, As)<sup>15,20</sup> were prepared according to the literature.

**Preparation of  $[\text{Rh}(\mu\text{-S-2-AsPh}_2\text{C}_6\text{H}_4\text{-}\kappa^2\text{S,As})_2\text{Rh}(\text{cod})]$  (**1**) and  $[\text{Rh}(\mu\text{-S-2-PPh}_2\text{C}_6\text{H}_4\text{-}\kappa^2\text{S,P})_2\text{Rh}(\text{cod})]$  (**2**).** A solution of ESH (0.62 mmol; E = As, P) and  $\text{NEt}_3$  (0.62 mmol) in ethanol (25 mL) was added to a suspension of  $[\{\text{RhCl}(\text{cod})\}_2]$  (0.32 mmol) in ethanol (15 mL). The reaction mixture was heated to reflux for 2½ h to give a dark red solution. The solution was concentrated to half its volume and the red solid that formed was separated by filtration, washed with methanol and dried in vacuo. Crystallisation from  $\text{CH}_2\text{Cl}_2$  at 8 °C yielded red crystals of **1** or **2**.

Data for **1**:

Yield: 0.22 g, 0.22 mmol (70%).

$^1\text{H}$  NMR ( $\delta$ , THF- $d_6$ ): 7.71 (d,  $^3J_{\text{HH}} = 8$  Hz, 4H, 2,6-H from Ph), 7.56 (d,  $^3J_{\text{HH}} = 8$  Hz, 2H, b-H from  $\text{C}_6\text{H}_4$ ), see Table 1 7.34 (t, 2H, 4-H from Ph), 7.30 (m, 6H, 3,5-H from Ph and e-H from  $\text{C}_6\text{H}_4$ ), 7.19 (t,  $^3J_{\text{HH}} = 8$  Hz, 2H, c-H from  $\text{C}_6\text{H}_4$ ), 7.09 (d,  $^3J_{\text{HH}} = 8$  Hz, 6H, 8,12-H and 10-H from Ph), 7.02 (t,  $^3J_{\text{HH}} = 8$  Hz, 2H, d-H from  $\text{C}_6\text{H}_4$ ), 6.89 (t,  $^3J_{\text{HH}} = 8$  Hz, 4H, 9,11-H from Ph), 4.37 (s, br, 2H, CH from cod), 2.81 (s, br, 2H, CH from cod), 2.49 (s, br, 2H,  $\text{CH}_2$  from cod), 1.92 (d, br, 4H,  $\text{CH}_2$  from cod), 1.54 (d, br, 2H,  $\text{CH}_2$  from cod).  $^{13}\text{C}\{^1\text{H}\}$  NMR ( $\delta$ , THF- $d_6$ ): 144.5 ( $\text{C}^a$ ), 142.8 ( $\text{C}^b$ ), 136.5 ( $\text{C}^c$ ), 135.0 ( $\text{C}^d$ ), 131.6 ( $\text{C}^e$ ,  $\text{C}^f$ ,  $\text{C}^g$ ), 129.8 ( $\text{C}^h$ ,  $\text{C}^{i2}$ ), 129.0 ( $\text{C}^e$ ), 127.3 ( $\text{C}^d$ ), 127.2 ( $\text{C}^d$ ), 126.4 ( $\text{C}^3$ ,  $\text{C}^5$ ,  $\text{C}^{10}$ ), 126.1 ( $\text{C}^9$ ,  $\text{C}^{11}$ ), 122.7 ( $\text{C}^e$ ), 76.8 (d,  $^1J_{\text{RhC}} = 13$  Hz, CH from cod), 72.4 (d,  $^1J_{\text{RhC}} = 12$  Hz, CH from cod), 29.6 ( $\text{CH}_2$  from cod), 28.2 ( $\text{CH}_2$  from cod).

IR (KBr,  $\text{cm}^{-1}$ ): 3048 (s), 2999 (m), 2933 (s), 2826 (s), 2872 (s), 2826 (s), 1953 (w), 1887 (w), 1809 (w), 1567 (s), 1480 (s), 1436 (vs), 1328 (m), 1304 (m), 1261 (m), 1246 (m), 1183 (m), 1157 (m), 1120 (m), 1078 (s), 1026 (m), 999 (m), 949 (w), 857 (m), 813 (w), 736 (vs), 715 (m), 693 (vs), 671 (m), 473 (vs), 445 (m), 424 (m).

EI MS,  $m/z$ : 988.0 (100%,  $\text{M}^+$ ).

Anal. Calcd: C 51.46, H 4.08, S 6.49. Found: C 51.60, H 4.73, S 6.54. Calcd. for  $\text{C}_{44}\text{H}_{40}\text{As}_2\text{Rh}_2\text{S}_2$ : M = 988.57.

M.p.: 255 °C (decomp.).

Data for **2**:

$^{31}\text{P}$  NMR ( $\delta$ , THF- $d_6$ ): 58.9 (d,  $^1J_{\text{RhP}} = 168$  Hz).

## General Procedure for the Hydrogenation of Olefins

The hydrogenation reactions were carried out in a stainless steel autoclave. THF and the substrate were added to a glass vessel containing a stirring bar and the rhodium complex **1**. The substrate/catalyst ratio was S/Rh = 200. The glass vessel was then transferred under nitrogen into the autoclave and the reaction mixture stirred under 10 bar  $\text{H}_2$  pressure at different temperatures and for different times. Afterwards, the reaction mixture was analysed by GC-MS.

## Data Collection and Structural Refinement of **1** and **2**

The data were collected on a Siemens CCD diffractometer (SMART) using  $\text{MoK}\alpha$  radiation ( $\lambda = 0.71073$  Å) and  $\omega$ -scan rotation. Data reduction was performed with SAINT including the program SADABS for empirical absorption correction. The structures were solved by direct methods, and the anisotropic refinement of all non-hydrogen atoms was performed with SHELX97. All H atoms for both structures are calculated on idealised positions. Structure figures were generated with ORTEP.<sup>21</sup>

CCDC 772937 (**1**) and 772938 (**2**) contain the supplementary crystallographic data for this paper. These data can be obtained free of charge from the Cambridge Crystallographic Data Centre via [www.ccdc.cam.ac.uk/data\\_request/cif](http://www.ccdc.cam.ac.uk/data_request/cif).

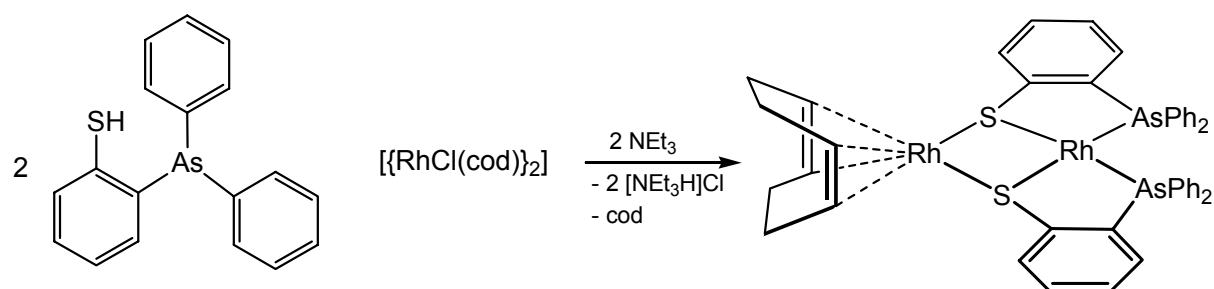
## RESULTS AND DISCUSSION

### Synthesis and spectroscopic properties of $[\text{Rh}(\mu\text{-S-2-EPh}_2\text{C}_6\text{H}_4\text{-}\kappa^2\text{S,As})_2\text{Rh}(\text{cod})]$ (**1**: E = As, **2**: E = P)

Treatment of one equivalent of  $[\{\text{RhCl}(\text{cod})\}_2]$  with two equivalents of the ligand 1-As $\text{Ph}_2$ -2-SHC $_6\text{H}_4$  (**AsSH**) in methanol in the presence of triethylamine as base (Eqn. 1) resulted in the formation of the dinuclear rhodium complex

$[\text{Rh}(\mu\text{-S-2-AsPh}_2\text{C}_6\text{H}_4\text{-}\kappa^2\text{S,As})_2\text{Rh}(\text{cod})]$  (**1**), in which the two rhodium centres are bridged by the sulfur atoms of two  $\text{AsS}^-$  ligands, and one 1,5-cyclooctadiene molecule is still coordinated. This

compound was isolated as red crystals and characterised by NMR and IR spectroscopy, MS and X-ray crystal structure analysis.



Eqn. 1

$^1\text{H}$  and  $^{13}\text{C}\{^1\text{H}\}$  NMR spectra of fresh solutions of **1** in  $\text{THF-d}_8$  showed the expected resonances corresponding to the aromatic hydrogen and carbon atoms, respectively, and a set of five signals (1:1:1:2:1) arising from the hydrogen atoms of the cyclooctadiene molecule. The proton and carbon resonances of **1** were assigned with the aid of two-dimensional NMR techniques (HMQC and  $^1\text{H},^1\text{H}$  COSY, Table 1).

The six sets of protons of the 1,5-cyclooctadiene molecule coordinated to rhodium give rise to an  $\text{AA}'\text{BB}'\text{CC}'\text{DD}'\text{EE}'\text{FF}'$  spin system. The individual signals were assigned with the aid of a  $^1\text{H},^1\text{H}$  COSY NMR spectrum (Fig. 1). The two-dimensional spectrum shows the connectivity of the non-equivalent ABCDEF protons. Due to coordination to rhodium and the symmetry of the molecule these protons give rise to five signals in a 1:1:1:2:1 ratio (Table 1).

Table 1

$^1\text{H}$  NMR chemical shifts for **1** ( $\delta$ ,  $\text{THF-d}_8$ )

	$\delta_{2,6} = 7.71$	$\delta_A = 4.37$
	$\delta_b = 7.56$	$\delta_B = 2.81$
	$\delta_4 = 7.34$	$\delta_C = 2.49$
	$\delta_{3,5,e} = 7.30$	$\delta_{D,E} = 1.92$
	$\delta_c = 7.19$	$\delta_F = 1.54$
	$\delta_{8,12,10} = 7.09$	
	$\delta_d = 7.02$	
	$\delta_{9,11} = 6.89$	

The  $^{13}\text{C}\{^1\text{H}\}$  NMR signals of  $\text{C}^A$  and  $\text{C}^B$  of the cyclooctadiene molecule (76.8 and 72.4 ppm) are split into doublets due to coupling with  $^{103}\text{Rh}$  and exhibit coupling constants of 13 and 12 Hz, respectively. The signals of the  $\text{CH}_2$  groups of cod appear at 29.6 and 28.2 ppm and thus indicate the inequivalence of these groups as observed in the  $^1\text{H}$  NMR spectrum.

The  $^1\text{H}$  NMR spectrum of **1** in  $\text{CDCl}_3$  indicates decomposition or dissociation in solution.

The mass spectrum (EI MS) of **1** showed the molecular ion  $[\text{M}]^+$  at  $m/z = 988$  as the most intense peak, with the corresponding isotopic

distribution. Another peak observed at  $m/z = 777$  indicates loss of the  $[\text{Rh}(\text{cod})]$  fragment.

The solid-state structure of the rhodium(I) carbonyl complex containing the phosphanylarylthiol 1- $\text{PPh}_2$ -2- $\text{S-C}_6\text{H}_4$  ( $\text{PS}^-$ ),  $[\text{Rh}\{\mu\text{-S-(PS)}-\kappa^2\text{S,P}\}(\text{CO})_2]$ , also shows a sulfur-bridged dimer (Fig. 2), which proved to be an efficient catalyst for the carbonylation of methanol to acetic acid.<sup>6</sup> Use of a large excess of ligand led to oxidation of  $\text{Rh}^{\text{I}}$  and isolation of a brown  $\text{Rh}^{\text{III}}$  complex, namely  $[\text{Rh}\{(\text{PS})-\kappa^2\text{S,P}\}_3]$ .<sup>22</sup> The use of  $[\text{RhCl}(\text{PPh}_3)_3]$  as a metal precursor led to formation of the same  $\text{Rh}^{\text{III}}$  complex.<sup>22</sup> The mixed-ligand  $\text{Ir}^{\text{III}}$  complex

$[\text{IrCl}_2\{(\text{PS})-\kappa^2\text{S},\text{P}\}(\text{PMe}_2\text{Ph})_2]$  has also been crystallographically characterised.<sup>22</sup> It is reported that the mononuclear  $\text{Rh}^{\text{I}}$  and  $\text{Ir}^{\text{I}}$  complexes

$[\text{M}\{(\text{PS})-\kappa^2\text{S},\text{P}\}(\text{CO})(\text{PPh}_3)]$  reversibly bind sulfur dioxide, and the iridium complex adds dihydrogen.<sup>23</sup>

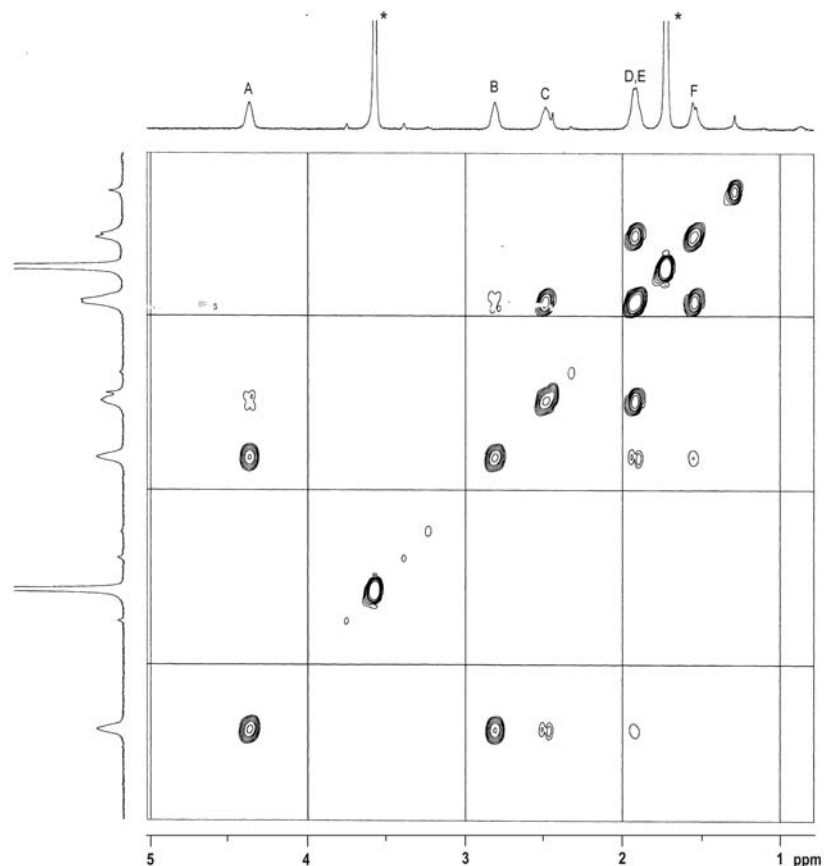


Fig. 1 –  $^1\text{H}, ^1\text{H}$  COSY NMR spectrum of **1** (aliphatic region, \*  $\text{THF-d}_8$ ).

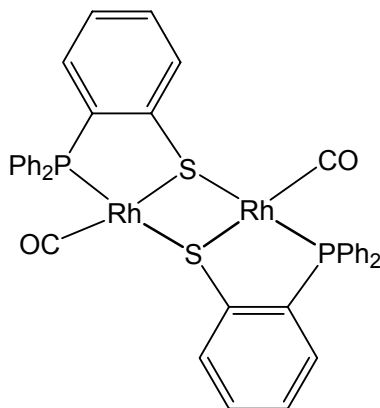


Fig. 2 – Schematic drawing of  $[\text{Rh}\{\mu\text{-S-(PS)-}\kappa^2\text{S},\text{P}\}(\text{CO})]_2$ .<sup>6</sup>

$[\text{M}\{\mu\text{-S-(PS)-}\kappa^2\text{S},\text{P}\}(\text{cod})]_2$  ( $\text{M} = \text{Rh}, \text{Ir}$ ) were prepared by reaction of  $\text{PS}^-$  with  $[\{\text{MCl}(\text{cod})\}_2]$ . However, based on the spectroscopic data, the complexes were assumed to be sulfur-bridged dimers like the carbonyl species (**Fig. 2**) with the 1,5-cyclooctadiene ligand acting as an  $\eta^2$  ligand.<sup>2</sup>

We synthesised the corresponding rhodium complex  $[\text{Rh}\{\mu\text{-S-(PS)-}\kappa^2\text{S},\text{P}\}_2\text{Rh}(\text{cod})]$  (**2**) with

the  $\text{PS}^-$  ligand using the same reaction conditions as for the  $\text{AsS}^-$  ligand. A few crystals of **2** were obtained from a  $\text{CH}_2\text{Cl}_2$  solution. An X-ray structure determination showed that the complex is also a sulfur-bridged dimer like **1**, with one 1,5-cyclooctadiene ligand coordinated in an  $\eta^4$  fashion. The  $^{31}\text{P}\{^1\text{H}\}$  NMR spectrum of **2** displays a doublet at 58.9 ppm with a  $^1J_{\text{RhP}}$  coupling constant

of 168 Hz. The  $^1\text{H}$  NMR spectrum shows a similar pattern of an AA'BB'CC'DD'EE'FF' spin system as in the case of **1**, however, the crystals were not pure enough to allow a full spectroscopical characterisation. Larger amounts of pure compound **2** have not been obtained up to now.

### Catalytic properties of **1** in the hydrogenation of olefins

Rhodium complex  $[\text{Rh}(\mu\text{-S-2-AsPh}_2\text{C}_6\text{H}_4\text{-}\kappa^2\text{S,As})_2\text{Rh}(\text{cod})]$  (**1**) was tested in the homogeneous hydrogenation of olefins in THF under 10 bar  $\text{H}_2$  with a substrate/rhodium ratio of 200. The olefins chosen for these tests were of the type  $\text{C}_6\text{H}_5\text{CH=CHR}$  ( $\text{R} = \text{H, Me, Ph, CHO}$ ), which contain a terminal C=C double bond, an internal C=C double bond, and both C=C and C=O double bonds, in order to test the selectivity for hydrogenation of internal C=C bonds rather than C=O bonds.

Complex **1** was active in the hydrogenation of styrene, and 100% conversion to ethylbenzene was observed after 3 h at 50 °C and 10 bar  $\text{H}_2$ . Hydrogenation of cod also occurs, as indicated by the presence of cyclooctane in the reaction mixture. Under the same reaction conditions (10 bar  $\text{H}_2$ , 50 °C) lower conversions were obtained for *trans*-methylstyrene (29%) and *trans*-stilbene (25%), after 16 h and 1 h, respectively, as expected for an olefin containing an internal C=C bond. The

GC-MS analysis of the product obtained from hydrogenation of cinnamaldehyde showed only selective hydrogenation of the C=C double bond in 13% conversion after 6 h at 50 °C. In conclusion, the comparative studies of the activity of **1** in hydrogenation reactions confirm that this rhodium complex with an As,S-containing ligand is active in the hydrogenation of olefins, and that it selectively hydrogenates the C=C double bond rather than the C=O bond in the case of cinnamaldehyde.

### Molecular structures of **1** and **2**

Red crystals of **1** and **2** suitable for X-ray diffraction analysis were obtained from a  $\text{CH}_2\text{Cl}_2$  solution by cooling to 8 °C. Compound **1** crystallises in the triclinic space group  $P\bar{1}$  with four molecules in the unit cell, and compound **2** in the monoclinic space group  $P2_1/n$  with four molecules in the unit cell. The two crystallographically independent molecules in the unit cell of **1** are nearly identical and shifted by 0.02/0.50/0.21 in *a/b/c* directions. However, all attempts to find a solution with a smaller unit cell failed. The asymmetric unit also contains four molecules of  $\text{CH}_2\text{Cl}_2$ . The discussion will be restricted to one of the two crystallographically independent molecules of **1**. Table 6 gives crystallographic details.

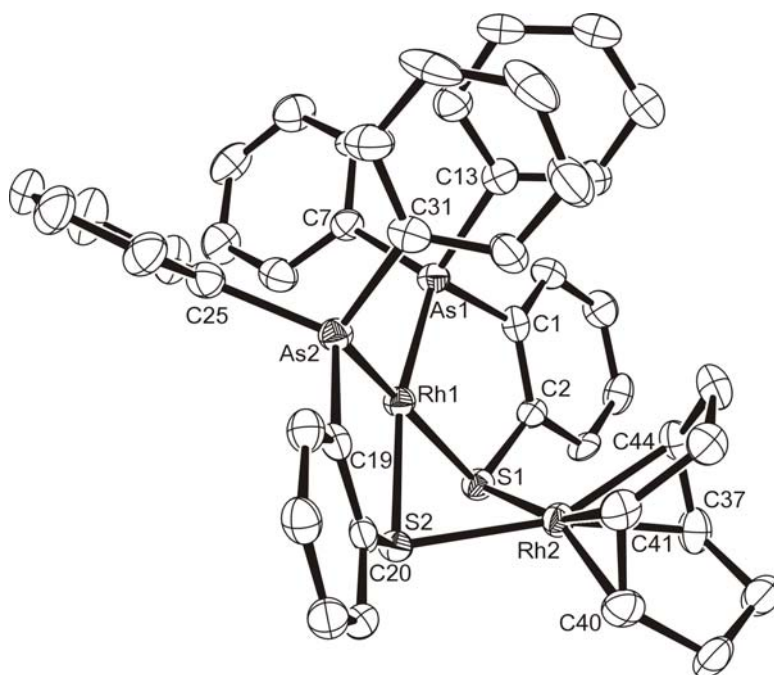


Fig. 3 – Solid-state molecular structure of **1** (30% probability ellipsoids, H atoms omitted for clarity).

The X-ray structure analysis shows for both compounds a dinuclear rhodium complex with two bridging S atoms from two arsanylarylthiolato or phosphanylarylthiolato ligands resulting in Rh<sub>2</sub>S<sub>2</sub> four-membered rings (Fig. 3). The structure of **1** is the first example of a dithiolato-bridged dirhodium complex with arsanylarylthiolato ligands. The two rhodium atoms are four-coordinate in a distorted square-planar geometry. Rh(1) is coordinated by two chelating AsS<sup>-</sup> or PS<sup>-</sup> ligands with formation of two RhECCS (E = As, P) five-membered rings. The coordination sphere of Rh(2) is completed by a cyclooctadiene molecule to give an approximately square-planar geometry [for **1**: S(2)–Rh(2)–Ct(1) 172.90°, S(1)–Rh(2)–Ct(2) 174.75°; for **2**: S(2)–Rh(2)–Ct(1) 175.07°, S(1)–Rh(2)–Ct(2) 173.45°, where Ct(1) and Ct(2) are the midpoints of the C(37)–C(44) and C(40)–C(41) bonds, respectively].

For complex **1**, the distance of rhodium to the midpoint of the coordinated double bond has a mean value of 2.01 Å and is in the usual range for rhodium(I) cod complexes.<sup>24–33</sup> Rh–C(olefinic) bond lengths are in the range 2.12(1)–2.16(1) Å. The Rh–S distances range from 2.290(3) to 2.405(3) Å and are slightly shorter for Rh(1) than for Rh(2). This difference is probably due to the presence of the two arylthiolato ligands bound to Rh(1) versus 1,5-cyclooctadiene on Rh(2). Nevertheless, they are in agreement with those observed in [Rh{(PS)-κ<sup>2</sup>S,P}(CO)]<sub>2</sub> and other dinuclear thiolato-bridged complexes.<sup>24–33</sup> The cyclooctadiene ring has a boat conformation with a mean C=C double-bond length of 1.395 Å. The lengths of the C–C single bonds are between 1.48(1) and 1.54(1) Å.

Selected bond lengths and bond angles for **1** and **2** are listed in Table 2.

Table 2

Selected experimental [calculated] bond lengths (Å) and bond angles (°) in **1** (E = As) and **2** (E = P)

Bond lengths			Bond angles			
	<b>1</b> <sup>a)</sup>	<b>2</b>	<b>1</b>		<b>2</b>	
Rh(1)–S(1)	2.290(3) [2.361]	2.3147(9) [2.376]	S(1)–Rh(1)–S(2)	80.5(1) [82.32]	80.18(3) [81.34]	
Rh(1)–S(2)	2.303(3) [2.369]	2.3257(9) [2.381]	S(1)–Rh(1)–E(1)	87.43(8) [87.03]	87.36(3) [87.30]	
Rh(1)–E(1)	2.325(1) [2.338]	2.2316(9) [2.243]	S(2)–Rh(1)–E(1)	166.53(8) [166.07]	166.49(3) [166.99]	
Rh(1)–E(2)	2.333(1) [2.337]	2.2251(9) [2.234]	S(1)–Rh(1)–E(2)	164.49(8) [165.56]	166.29(3) [166.19]	
Rh(2)–C(44)	2.12(1) [2.108]	2.119(3) [2.106]	S(2)–Rh(1)–E(2)	87.49(8) [86.63]	87.72(3) [87.12]	
Rh(2)–C(40)	2.13(1) [2.109]	2.123(3) [2.110]	E(1)–Rh(1)–E(2)	103.34(5) [102.25]	103.99(3) [103.20]	
Rh(2)–C(41)	2.14(1) [2.120]	2.121(3) [2.116]	S(1)–Rh(2)–S(2)	76.53(9) [77.82]	76.70(3) [77.32]	
Rh(2)–C(37)	2.16(1) [2.123]	2.139(3) [2.124]	C(44)–Rh(2)–C(40)	97.9(5) [99.02]	98.3(1) [99.05]	
Rh(2)–S(1)	2.386(3) [2.480]	2.4208(8) [2.486]	C(44)–Rh(2)–C(41)	81.8(4) [82.57]	82.8(1) [82.76]	
Rh(2)–S(2)	2.405(3) [2.477]	2.3954(9) [2.477]	C(40)–Rh(2)–C(41)	38.7(4) [39.18]	38.5(1) [39.23]	
E(1)–C(13)	1.94(1) [1.948]	1.840(3) [1.833]	C(44)–Rh(2)–C(37)	37.7(4) [39.15]	38.3(1) [39.15]	
E(1)–C(7)	1.96(1) [1.952]	1.828(3) [1.837]	C(40)–Rh(2)–C(37)	81.6(5) [81.69]	81.4(1) [81.64]	
E(1)–C(1)	1.97(1) [1.948]	1.848(3) [1.841]	C(41)–Rh(2)–C(37)	89.9(5) [90.74]	90.4(1) [90.88]	
E(2)–C(25)	1.94(1) [1.946]	1.835(3) [1.829]	C(44)–Rh(2)–S(1)	95.4(3) [95.75]	95.17(9) [95.88]	
E(2)–C(31)	1.95(1) [1.944]	1.835(3) [1.832]	C(40)–Rh(2)–S(1)	158.4(3) [156.34]	160.1(1) [156.77]	
E(2)–C(19)	1.95(1) [1.944]	1.841(3) [1.838]	C(41)–Rh(2)–S(1)	161.6(3) [162.90]	159.3(1) [162.11]	
S(1)–C(2)	1.76(1) [1.781]	1.779(3) [1.776]	C(37)–Rh(2)–S(1)	99.0(3) [98.69]	100.77(9) [99.32]	
S(2)–C(20)	1.78(1) [1.782]	1.780(3) [1.777]	C(44)–Rh(2)–S(2)	155.8(3) [159.22]	158.6(1) [159.27]	
			C(40)–Rh(2)–S(2)	97.2(3) [93.95]	95.1(1) [94.01]	
			C(41)–Rh(2)–S(2)	98.7(3) [97.75]	97.8(1) [97.69]	
			C(37)–Rh(2)–S(2)	164.9(4) [160.66]	162.0(1) [160.57]	
			Rh(1)–S(1)–Rh(2)	76.38(8) [71.70]	74.29(2) [71.34]	
			Rh(1)–S(2)–Rh(2)	75.76(8) [71.61]	74.58(3) [71.41]	

a) data are given for one of the two crystallographically independent molecules only

The two  $\text{AsS}^-$  and  $\text{PS}^-$  ligands coordinated to Rh(1) are in a *cis* arrangement and slightly folded toward each other [S(2)–Rh(1)–E(1) 166.53(8)° (1), 166.49(3)° (2); S(1)–Rh(1)–E(2) 164.49(8)° (1), 166.29(3)° (2)]. This results in a distorted square-planar geometry at Rh(1) (distance of Rh(1) to the As(1)–S(1)–As(2)–S(2) plane: 0.175 Å in 1,

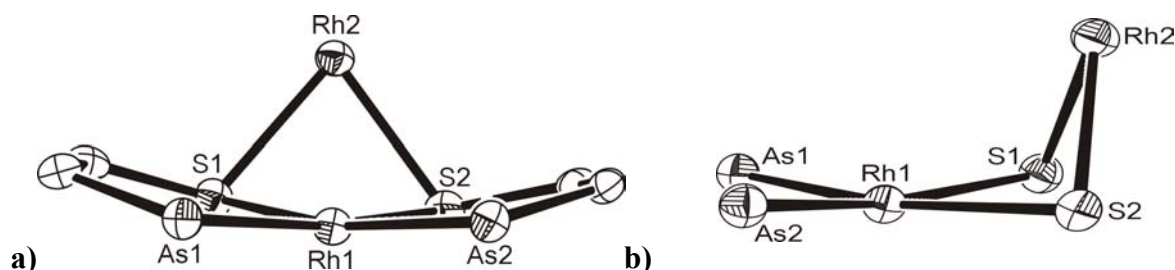


Fig. 4 – Structure fragments of **1** showing a) the distorted square-planar arrangement around Rh(1) and b) the bent Rh(1)S(1)Rh(2)S(2) ring.

The  $\text{Rh}_2\text{S}_2$  ring is bent along the S...S vector with a dihedral angle of 105.4° in **1** and 102.6° in **2** between the  $\text{RhS}_2$  planes (Fig. 4b) (cf. 112.7° in  $[\text{Rh}\{\mu\text{-S}(\text{PS})\text{-}\kappa^2\text{S},\text{P}\}(\text{CO})_2\}_2$ )<sup>6</sup>. The puckering of the  $\text{Rh}_2\text{S}_2$  core leads to short Rh...Rh distances of 2.892(1) Å in **1** and 2.8608(5) Å in **2**, which are at the lower end of the typical range for thiolato-bridged  $\text{Rh}^{\text{I}}$  complexes [ $d(\text{Rh}\cdots\text{Rh}) = 2.87\text{--}3.52$  Å; 2.980(1) Å for the carbonyl complex  $[\text{Rh}\{\mu\text{-S}(\text{PS})\text{-}\kappa^2\text{S},\text{P}\}(\text{CO})_2\}_2$ ]<sup>6,24–40</sup>. In some of these cases short metal–metal interactions have been confirmed by theoretical calculations.<sup>27</sup> For instance, a theoretical and structural study on binuclear square-planar complexes of  $d^8$  transition metal ions  $[\text{L}^{\text{A}}_2\text{M}(\mu\text{-X})_2\text{ML}^{\text{B}}_2]$  (X = Cl, Br, I;  $\text{L}^{\text{A}} = \text{L}^{\text{B}} = \text{PH}_3, \text{PF}_3, \text{CO}, \text{Cl}$ ;  $\text{L}^{\text{A}} = \text{PH}_3, \text{Me}$ ,  $\text{L}^{\text{B}} = \text{PH}_3, \text{Me}$ ) focussed on elucidating the factors that

Fig. 4a, Table 2). The As–Rh–S chelate angles [87.43(8)° and 87.49(8)°] are comparable to the P–Rh–S chelate angles found in complex **2** [87.36(3)°, 87.72(3)°], and are in accord with the preferred P–M–S bite angles observed for these ligands.<sup>2</sup>

determine the degree of bending in such compounds.<sup>41</sup> For different metal atoms the stability of the bent form increases in the order  $\text{Ni}^{\text{II}} < \text{Pd}^{\text{II}} < \text{Pt}^{\text{II}} < \text{Rh}^{\text{I}} < \text{Ir}^{\text{I}}$ . A driving force for bending of the molecules appears to be the donor–acceptor interactions between the  $d_{z^2}$  electrons and empty  $p_z$  orbitals of the two metal atoms. The metal...metal interaction is modulated by the nature of the metal atom, the terminal ligands and the bridging atoms.<sup>41</sup> Thus, for face-to-face  $\text{M}_2\text{L}_8$  dimers of type a (Fig. 5) the metal...metal bonding interaction results from the combined effect of the repulsion between the electrons in the  $d_{z^2}$  orbitals of the  $\text{ML}_4$  monomers and the donor–acceptor interactions between the  $d_{z^2}$  electrons and the empty  $p_z$  orbitals.<sup>41–43</sup>

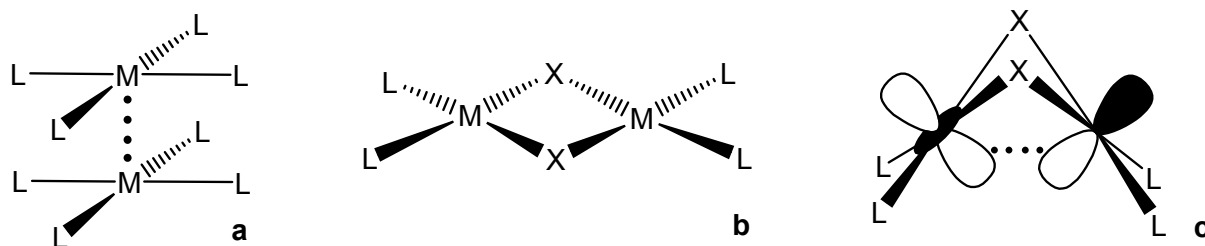


Fig. 5 – Metal...metal interaction in transition metal dimers.<sup>41–43</sup>

In planar dimers (type b, Fig. 5) these interactions may become significant when the dimer is bent along the X...X vector (type c, Fig. 5). However, only for large degrees of bending is the M...M interaction attractive enough to make the molecule more stable in its bent form ( $\theta < 140^\circ$ ,

fold angle, defined as the dihedral angle between the coordination planes of the two metal centres). The energy difference between the planar and the bent form is on the order of 10 kcal/mol, and steric effects seem to be important in preventing bending only for bulky terminal ligands.<sup>41</sup> However,

packing effects in the crystal may also be considered to play an important role in the degree of folding of the molecule.<sup>44</sup>

### Theoretical Studies

Geometry optimisations were carried out with the Gaussian 09 suite of programs,<sup>45</sup> using the M06-L pure functional,<sup>46</sup> which is known to give accurate results for transition metal compounds at low computational cost<sup>47</sup>. All calculations were performed by using the DZQ basis set recommended by Schultz *et al.*<sup>48</sup> for the rhodium atoms, the standard 6-31G(d,p) basis for As, P, S and C, and 6-31G for hydrogen. The DZQ basis set

uses the relativistic effective core potentials (ECP) of Stevens *et al.*,<sup>49–50</sup> along with a valence electron basis set of the (8s8p6d)/[4s4p3d] size.<sup>51</sup>

Both geometries obtained from the X-ray diffraction data and geometries with the fold angle  $\theta$  constrained to 180° were optimised. The calculated parameters for the bent structures are in excellent agreement with the experimental values (Table 2). As expected, in both cases the planar forms lie at significantly higher relative energies. The energy difference between the bent and planar structures is around 30.65 kcal mol<sup>-1</sup> (Table 3), higher than the range predicted for similar, but simpler dinuclear complexes.<sup>41</sup> None of the structures exhibited imaginary frequencies.

Table 3

Relative energies, with ZPE correction and calculated Rh···Rh distances, for the bent and planar geometries of **1** and **2**

	Fold angle $\theta$ [°]	Rel. $E$ [kcal mol <sup>-1</sup> ]	Rh···Rh distance [Å]
1	99.70	0	2.837
	180.00	30.96	3.643
2	98.52	0	2.837
	180.00	30.34	3.614

The total electron densities (0.04 e a.u.<sup>-13</sup>) of both bent and planar structures were calculated for **1** (Fig. 6), in order to determine whether there is an interaction or not between the rhodium atoms. In the bent form, considerable electron density associated with the Rh···Rh vector indicates an interaction between the two atoms. On the other hand, in the planar form, there is a lack of electron density between the two rhodium atoms. The

electron density of **2** exhibits the same distribution as in **1**.

Since it was predicted that d→p\* donor–acceptor interactions between the two metal atoms make the main contribution to bending of these compounds,<sup>41</sup> natural bond orbital (NBO) calculations were performed with the NBO code<sup>52</sup> included in Gaussian 09 in order to identify them.

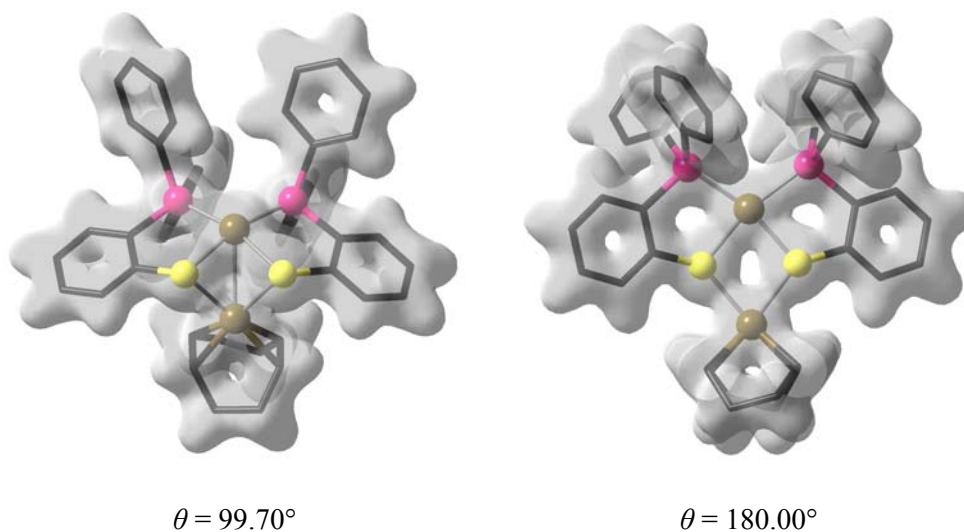


Fig. 6 – Total electron density surfaces (0.04 e a.u.<sup>-13</sup>) for the bent and planar form of **1** (C: black, S: yellow, As: violet, Rh: brown).



Several  $d \rightarrow p^*$  interactions between the occupied orbitals ( $n$ ) of one Rh atom and the unoccupied orbitals ( $n^*$ ) of the other Rh atom were identified for the bent structures in **1** and **2**. The occupancy and character of these Rh natural bond orbitals (NBOs) are given in Tables 4 and 5, along with the associated second-order energy-lowering values ( $\Delta E^{(2)}$ ), which estimate the degree of donor–acceptor interaction.<sup>52</sup> In the case of the bent structure not only the  $d_z^2$ , but also the other d-type

orbitals interact with the empty  $p^*$  orbitals (Fig. 7). Since these interactions are no longer present in the planar structures in **1** and **2**, they must play an important additional role in the stabilisation of the bent forms and may explain the higher relative energy differences compared to those found in the literature for simpler dinuclear model complexes. The  $d_z^2 \rightarrow p^*$  interactions are also present in the planar structures, but with significantly lower  $\Delta E^{(2)}$  values.

Table 4

 Calculated NBOs on the two Rh atoms of **1**

$\theta$ [°]	Donor NBO	Occupancy	d character [%]	Acceptor NBO	Occupancy	p character [%]	$\Delta E^{(2)}$ [kcal/mol]
99.70	$n_{Rh(1)}$	1.97	99.5	$n_{Rh(2)}^*$	0.10	98.3	16.06
	$n_{1 Rh(2)}$	1.92	99.5	$n_{1 Rh(2)}^*$	0.14	95.2	13.59
				$n_{2 Rh(2)}^*$	0.11	97.1	13.05
	$n_{2 Rh(2)}$	1.90	98.4	$n_{1 Rh(2)}^*$	0.14	95.2	28.42
$n_{2 Rh(2)}^*$				0.11	97.1	30.18	
$n_{3 Rh(2)}$	1.89	99.4	$n_{1 Rh(2)}^*$	0.14	95.2	12.37	
			$n_{2 Rh(2)}^*$	0.11	97.1	13.34	
180.00	$n_{Rh(1)}$	1.98	99.2	$n_{Rh(2)}^*$	0.22	75.2	6.11
	$n_{Rh(2)}$	1.97	98.8	$n_{Rh(1)}^*$	0.19	89.8	8.4

Table 5

 Calculated NBOs on the two Rh atoms of **2**

$\theta$ [°]	Donor NBO	Occupancy	d character [%]	Acceptor NBO	Occupancy	p character [%]	$\Delta E^{(2)}$ [kcal/mol]
98.52	$n_{1 Rh(1)}$	1.92	99.40	$n_{1 Rh(2)}^*$	0.14	93.26	20.92
				$n_{2 Rh(2)}^*$	0.11	98.36	19.81
	$n_{2 Rh(1)}$	1.90	99.14	$n_{1 Rh(2)}^*$	0.14	93.26	10.56
				$n_{2 Rh(2)}^*$	0.11	98.36	20.46
	$n_{3 Rh(1)}$	1.90	99.50	$n_{2 Rh(2)}^*$	0.11	98.36	6.82
	$n_{4 Rh(1)}$	1.87	99.54	$n_{1 Rh(2)}^*$	0.14	93.26	6.86
				$n_{2 Rh(2)}^*$	0.11	98.36	9.76
$n_{1 Rh(2)}$	1.97	99.36	$n_{1 Rh(1)}^*$	0.20	87.22	16.64	
			$n_{2 Rh(1)}^*$	0.10	97.33	20.39	
$n_{2 Rh(2)}$	1.63	98.50	$n_{1 Rh(1)}^*$	0.20	87.22	13.24	
			$n_{2 Rh(1)}^*$	0.10	97.33	7.92	
$n_{3 Rh(2)}$	1.59	98.56	$n_{1 Rh(1)}^*$	0.20	87.22	25.39	
			$n_{2 Rh(1)}^*$	0.10	97.33	18.28	
180.00	$n_{Rh(1)}$	1.96	98.90	$n_{Rh(2)}^*$	0.15	96.43	7.23
	$n_{Rh(2)}$	1.98	99.28	$n_{Rh(1)}^*$	0.19	81.27	9.4

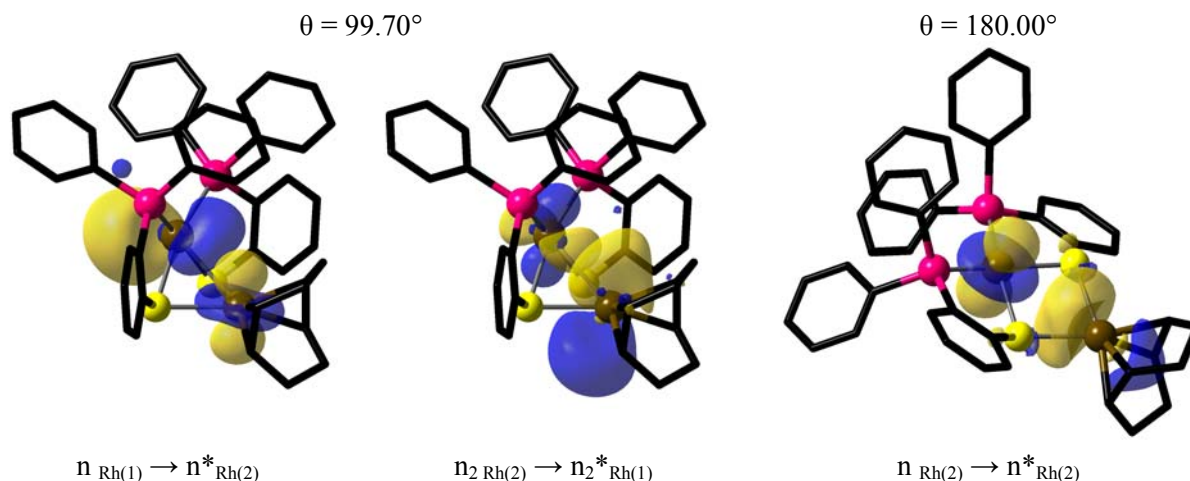


Fig. 7 – Contours of some relevant NBOs of **1**. Positive values of the orbital contour are represented in yellow (0.05 au) and negative values in blue (–0.05 au). (For the interpretation of the references to colour in this legend, the reader is referred to the web version of this article).

Table 6

Crystallographic data for **1** and **2**

	<b>1</b>	<b>2</b>
Empirical formula	C <sub>44</sub> H <sub>40</sub> As <sub>2</sub> Rh <sub>2</sub> S <sub>2</sub> ·2 CH <sub>2</sub> Cl <sub>2</sub>	C <sub>44</sub> H <sub>40</sub> P <sub>2</sub> Rh <sub>2</sub> S <sub>2</sub>
Formula weight	1158.39	900.64
Temperature	210(2) K	213(2) K
Crystal system	triclinic	monoclinic
Space group	<i>P</i> $\bar{1}$	<i>P</i> 2 <sub>1</sub> / <i>n</i>
Unit cell dimensions	<i>a</i> = 10.752(3) Å <i>b</i> = 20.625(7) Å <i>c</i> = 21.042(7) Å $\alpha$ = 79.028(5)° $\beta$ = 88.216(6)° $\gamma$ = 79.103(6)°	<i>a</i> = 12.801(2) Å <i>b</i> = 19.390(2) Å <i>c</i> = 15.068(2) Å $\beta$ = 96.443(2)°
Volume	4498(2) Å <sup>3</sup>	3716.6(8) Å <sup>3</sup>
<i>Z</i>	4	4
Density (calculated)	1.711 Mg/m <sup>3</sup>	1.610 Mg/m <sup>3</sup>
Absorption coefficient	2.557 mm <sup>-1</sup>	1.119 mm <sup>-1</sup>
F(000)	2304	1824
Crystal size	0.20 × 0.20 × 0.04 mm	0.20 × 0.10 × 0.03 mm
$\Theta_{\text{Min}}/\Theta_{\text{Max}}$	1.93/26.37°	1.72/28.37°
Index ranges	–13 ≤ <i>h</i> ≤ 12, –25 ≤ <i>k</i> ≤ 25, –26 ≤ <i>l</i> ≤ 26	–17 ≤ <i>h</i> ≤ 16, –22 ≤ <i>k</i> ≤ 25, –19 ≤ <i>l</i> ≤ 19
Reflections collected	41402	26556
Independent reflections	18152 [ <i>R</i> (int) = 0.0562]	8710 [ <i>R</i> (int) = 0.0385]
Completeness to $\Theta_{\text{Max}}$	98.6 %	93.9 %
Refinement method	full-matrix least-squares on <i>F</i> <sup>2</sup>	full-matrix least-squares on <i>F</i> <sup>2</sup>
Restraints / Parameters	18/1010	0/451
Goodness-of-fit on <i>F</i> <sup>2</sup>	1.090	1.069
Final <i>R</i> indices [ <i>I</i> > 2σ( <i>I</i> )]	<i>R</i> 1 = 0.0769, <i>wR</i> 2 = 0.1822	<i>R</i> 1 = 0.0426, <i>wR</i> 2 = 0.0658
<i>R</i> indices (all data)	<i>R</i> 1 = 0.1432, <i>wR</i> 2 = 0.2218	<i>R</i> 1 = 0.0648, <i>wR</i> 2 = 0.0705
Largest diff. peak and hole	2.341 and –1.380 eÅ <sup>-3</sup>	0.554 and –0.445 eÅ <sup>-3</sup>

**Acknowledgements:** We gratefully acknowledge financial support from the International Postgraduate Programme (IPP “Research at the Frontiers of Chemistry”) at the University of Leipzig and the Deutscher Akademischer Austausch Dienst (DAAD, SOE programme) (A.H.) and the EU-COST Action CM0802 “PhoSciNet”. The theoretical part of this work was undertaken with financial support provided from programs co-financed by the Sectoral Operational Programme Human Resources Development, Contract POSDRU 6/1.5/S/3 –

“Doctoral studies: through science towards society” and from the CMMCCC 130/2007 program, Roumania (M.B.S.).

## REFERENCES

1. A. Bader and E. Linder, *Coord. Chem. Rev.*, **1991**, *108*, 27-110.
2. J. R. Dilworth and N. Wheatley, *Coord. Chem. Rev.*, **2000**, *199*, 89-158 and refs. therein.

3. C. S. Slone, D. A. Weinberger and C. A. Mirkin, *Prog. Inorg. Chem.*, **1999**, *48*, 233-350.
4. P. Braunstein and F. Naud, *Angew. Chem., Int. Ed. Engl.*, **2001**, *40*, 680-699.
5. E. Hauptman, R. Shapiro and W. Marshall, *Organomet.*, **1998**, *17*, 4976-4982; P. Barbaro, A. Currao, J. Herrmann, R. Nesper, P. S. Pregosin and R. Salzmann, *Organomet.*, **1996**, *15*, 1879-1888; M. Tschoerner, G. Trabesinger, A. Albinati and P. S. Pregosin, *Organomet.*, **1997**, *16*, 3447-3453; A. Albinati, J. Eckert, P. Pregosin, H. Rüegger, R. Salzmann and C. Stössel, *Organomet.*, **1997**, *16*, 579-590; S. Gladiali, A. Dore and D. Fabbri, *Tetrahedron: Asymm.*, **1994**, *5*, 1143-1146; M. Bressan, C. Bonuzzi, F. Morandini and A. Morvillo, *Inorg. Chim. Acta*, **1991**, *182*, 153-156; M. Hiraoka, A. Nishikawa, T. Morimoto and K. Achiwa, *Chem. Pharm. Bull.*, **1998**, *46*, 704-706.
6. J. R. Dilworth, J. R. Miller, N. Wheatley, M. J. Baker and J. G. Sunley, *J. Chem. Soc., Chem. Commun.*, **1995**, 1579-1581.
7. N. Khair, B. Suárez, V. Valdivia, I. Fernández, *Synlett*, **2005**, *19*, 2963-2967.
8. R. Malacea, E. Manoury, L. Routaboul, J. C. Daran, R. Poli, J. P. Dunne, A. C. Withwood, C. Godard and S. B. Duckett, *Eur. J. Inorg. Chem.*, **2006**, 1803-1816.
9. W. Zeng and Y.-G. Zhou, *Tetrahedron Lett.*, **2007**, *48*, 4619-4622.
10. H. Y. Cheung, W.-Y. Yu, F. L. Lam, T. T.-L. Au-Yeung, Z. Zhou, T. H. Chan and A. S. C. Chan, *Org. Lett.*, **2007**, *9*, 4295-4298.
11. F. L. Lam, T. T.-L. Au-Yeung, F. Y. Kwong, Z. Zhou, K. Y. Wong and A. S. C. Chan, *Angew. Chem. Int. Ed.*, **2008**, *47*, 1280-1283.
12. M. Kato, T. Nakamura, K. Ogata, and S. Fukuzawa, *Eur. J. Org. Chem.*, **2009**, 5232-5238.
13. X. Caldenty and M. A. Pericàs, *J. Org. Chem.*, **2010**, *75*, 2628-2644.
14. (a) G. D. Figuly, C. K. Loop and J. C. Martin, *J. Am. Chem. Soc.*, **1989**, *111*, 654-658; (b) E. Block, V. Eswarakrishnan, M. Gernon, G. Ofori-Okai, C. Saha, K. Tang and J. Zubieta, *J. Am. Chem. Soc.*, **1989**, *111*, 658-665; (c) K. Smith, C. M. Lindsay and G. J. Pritchard, *J. Am. Chem. Soc.*, **1989**, *111*, 665-669.
15. E. Block, G. Ofori-Okai and J. Zubieta, *J. Am. Chem. Soc.*, **1989**, *111*, 2327-2329.
16. J. K. Dunleavy, *Platinum Metals Rev.*, **2006**, *50*, 110-110; D. E. Grove, *Platinum Metals Rev.*, **2003**, *47*, 44-44.
17. G. B. D. Rousseau, N. Bovet and M. Kadodwala, *J. Phys. Chem. B*, **2006**, *110*, 21857-21564; G. J. Hutchings, F. King, I. P. Okoye, M. B. Padley and C. H. Rochester, *J. Catal.*, **1994**, *148*, 453-463.
18. G. Giordano and R. H. Crabtree, *Inorg. Synth.*, **1990**, *28*, 88-90.
19. F. F. Blicke and F. D. Smith, *J. Chem. Soc.*, **1929**, *51*, 1558-1565.
20. A. Hildebrand, PhD Thesis, Universität Leipzig/"Babes-Bolyai" University, **2006**.
21. (a) SMART: Area-Detector Software Package, 1993, Siemens Industrial Automation, Inc., Madison, WI; (b) SAINT: Area-Detector Integration Software. Version 6.01 (1999) Siemens Industrial Automation, Inc.: Madison, WI; (c) SADABS: G.M. Sheldrick, SADABS, Program for Scaling and Correction of Area-detector Data, Göttingen, **1997**; (d) SHELX97 [Includes SHELXS97, SHELXL97]: G.M. Sheldrick, (**1997**). SHELX97. Programs for Crystal Structure Analysis (Release 97-2), University of Göttingen, Germany; (e) ORTEP3 for Windows: L. J. Farrugia, *J. Appl. Cryst.*, **1997**, *30*, 565-566.
22. J. R. Dilworth, C. Lu, J. R. Miller and Y. Zheng, *J. Chem. Soc., Dalton Trans.*, **1995**, 1957-1964.
23. L. Dahlenburg, K. Herbst and M. Kühnlein, *Z. Anorg. Allg. Chem.*, **1997**, *623*, 250-258.
24. R. Hill, B. A. Kelly, F. G. Kennedy, S. A. Knox and P. Woodward, *J. Chem. Soc., Chem. Commun.*, **1977**, 434-436.
25. T. A. Wark and D. W. Stephan, *Can. J. Chem.*, **1990**, *68*, 565-569.
26. M. A. Ciriano, J. Pérez-Torrente, F. J. Lahoz and L. A. Oro, *J. Chem. Soc. Dalton Trans*, **1992**, 1831-1837.
27. A. M. Masdeu, A. Ruiz, S. Castellón, C. Claver, P. B. Hitchcock, P. A. Chaloner, C. Bó, J. M. Poblet and P. Sarasa, *J. Chem. Soc. Dalton Trans*, **1993**, 2689-2696.
28. H. Brunner, J. Bügler and B. Nuber, *Tetrahedron: Asymm.*, **1996**, *7*, 3095-3098.
29. R. Fandos, M. Martínez-Ripoll, A. Otero, M. J. Ruiz, A. Rodriguez and P. Terreros, *Organometallics*, **1998**, *17*, 1465-1470.
30. A. Polo, C. Claver, S. Castellón, A. Ruiz, J. C. Bayón, J. Real, C. Mealli and D. Masi, *Organometallics*, **1992**, *11*, 3525-3533.
31. D. Cruz-Garriz, B. Rodriguez, H. Torrens and J. Leal, *Trans. Met. Chem.*, **1984**, *9*, 284-285.
32. A. Elduque, C. Finestra, J. A. López, F. J. Lahoz, F. Merchán, L. A. Oro and M. T. Pinillos, *Inorg. Chem.*, **1998**, *37*, 824-829.
33. J. R. Dilworth, D. Morales and Y. Zheng, *J. Chem. Soc., Dalton Trans*, **2000**, 3007-3015.
34. J. J. Bonnet, P. Kalck and R. Poilblanc, *Inorg. Chem.*, **1977**, *16*, 1514-1518.
35. J. J. Bonnet, A. Thorez, A. Maisonnat, J. Galy and R. Poilblanc, *J. Am. Chem. Soc.*, **1979**, *101*, 5940-5949.
36. R. Choukroun, D. Gervais, J. Jaud, P. Kalck and F. Senocq, *Organometallics*, **1986**, *5*, 67-71.
37. C. Claver, P. Kalck, M. Ridmy, A. Thorez, L. A. Oro, M. T. Pinillos, M. C. Apreta, F. H. Cano and C. Foces-Foces, *J. Chem. Soc., Dalton Trans*, **1988**, 1523-1528.
38. C. Claver, A. M. Masdeu, N. Ruiz, C. Foces-Foces, F. H. Cano, M. C. Apreta, L. A. Oro, J. Garcia-Alejandre and H. Torrens, *J. Organomet. Chem.*, **1990**, *398*, 177-186.
39. A. Polo, E. Fernandez, C. Claver and S. Castellón, *J. Chem. Soc., Chem. Commun.*, **1992**, 639-640.
40. J. R. Dilworth, J. R. Miller, N. Wheatley, M. J. Baker and J. G. Sunley, *J. Chem. Soc., Chem. Commun.*, **1995**, 1579-1581.
41. G. Aullón, G. Ujaque, A. Lledós, S. Alvarez and P. Alemany, *Inorg. Chem.*, **1998**, *37*, 804-813.
42. J. Novoa, G. Aullón, P. Alemany and S. Alvarez, *J. Am. Chem. Soc.*, **1995**, *117*, 7169-7171.
43. G. Aullón, P. Alemany and S. Alvarez, *Inorg. Chem.*, **1996**, *35*, 5061-5067.
44. P. Hofmann, C. Meier, W. Hiller, M. Heckel, J. Riede and M. U. Schmidt, *J. Organomet. Chem.*, **1995**, *490*, 51-70.

45. M. J. Frisch *et al.*, *Gaussian 09, Revision A.02*; Gaussian, Inc., Wallingford CT, **2009**.
46. Y. Zhao and D. G. Truhlar, *J. Chem. Phys.*, **2006**, *125*, 194101-194118.
47. Y. Zhao and D. G. Truhlar, *Acc. Chem. Res.*, **2008**, *41*, 157-167.
48. N. E. Schultz, Y. Zhao and D. G. Truhlar, *J. Phys. Chem. A*, **2005**, *109*, 11127-11143.
49. W. J. Stevens, H. Basch and M. Krauss, *J. Chem. Phys.*, **1984**, *81*, 6026-6033.
50. T. R. Cundari and W. J. Stevens, *J. Chem. Phys.*, **1993**, *98*, 5555-5565.
51. N. E. Schultz, Y. Zhao and D. G. Truhlar, *J. Phys. Chem. A*, **2005**, *109*, 4388-4403.
52. A. E. Reed, L. A. Curtiss and F. Weinhold, *Chem. Rev.*, **1988**, *88*, 899-926.